Recycling-Oriented Investigation of Local Porosity Changes in Microwave Heated-Concrete

Nicholas Lippiatt, Florent Bourgeois

Recycling-Oriented Investigation of Local Porosity Changes in Microwave Heated-Concrete†

Nicholas R. Lippiatt and Florent S. Bourgeois*

[1] *Laboratoire de Génie Chimique UMR CNRS 5503, Université de Toulouse, France*

Abstract

Large quantities of concrete waste are being produced continuously throughout the world, of which only a fraction are downcycled as construction backfill or as road-base. Seeking total concrete recyclability, this work concerns the development of microwave-based solutions for the separation of individual constituents of concrete. By focusing on the interaction between microwaves and concrete at the microscopic level, the paper makes important connections between local changes in the microwave-heated concrete texture and macroscopic changes in mechanical properties. Through analysis of the concrete texture using SEM imaging, it is found that the microwave heating of concrete causes fracture porosity. The size and shape of fracture porosity can be correlated with recycling performance indicators; namely aggregate liberation, concrete strength and product fineness. In particular, the work finds that only a short exposure to microwaves promotes the formation of a primary fracture network responsible for selective liberation of aggregates. Longer exposure to microwave heating creates a secondary network of smaller fractures that spreads throughout the cement phase, which is directly associated with the changes in mechanical strength of concrete and product fineness.

The work introduces the concept of textural versus physical liberation, and shows that while microwave heating creates a high selective textural liberation of aggregate particles, the comminution of microwave-heated concrete may not necessarily yield high physical liberation. The work concludes that the key to designing a microwave-based process for concrete recycling resides in finding comminution and separation technologies that can best harvest the benefits of the textural and mechanical changes produced by microwave heating.

Keywords: concrete, recycling, microwave heating, fracture porosity

1. Introduction

Concrete is the most-used manufactured product on the planet, as a consequence it also constitutes a large fraction of urban waste. Many countries already make use of concrete waste as backfill and road base. Countries such as the Netherlands and Denmark manage to recycle over 80% of the construction and demolition (C&D) waste they generate (Fischer and Davidsen, 2011; Symonds, 1999). Nonetheless, a large fraction of concrete waste is not used and the concrete that is recycled is invariably downcycled, as can be seen by the ratio of virgin aggregate to recycled aggregate used in concrete production (Klee, 2009). Using crushed concrete as a replacement for coarse aggregate reduces the mechanical performance of the final product in proportion with the fraction of crushed concrete used. This effect is significantly greater when crushed concrete is used as a replacement for fine aggregates, which is why concrete waste is almost never used in this way. The reason crushed concrete reduces the performance of concrete compared to virgin aggregate appears to be due to adhered cement paste and how it reacts to new cement as it cures (Tam et al., 2007). The first step to complete concrete recyclability therefore is finding an effective technique to decrease the volume of adhered cement on recycled aggregates.

Microwave heating is especially applicable to processing multiphase materials as it uses the differences in thermal and dielectric properties between distinct phases to generate fractures and weaken the material. A simple version of this scenario is a strongly dielectric material embedded in a continuous microwave transparent material. In fact, this basic scenario closely resembles what is found for mineral ores, for which microwave heating as a companion treatment step before crushing and milling has been considered for some time and has been shown to weaken the ore and increase mineral liberation, hence mineral yield (Kingman et al., 2004a). The ever-present question is whether the benefit of the increased yield

† Accepted: August 20, 2013

[1] CNRS-Laboratoire de Génie Chimique UMR 5503, 4 Allée Emile Monso BP 84234, 31432 Toulouse Cedex 4, France

* Corresponding author:
E-mail: florent.bourgeois@inp-toulouse.fr
TEL: +33-534-323-633 FAX: +33-534-323-700

exceeds the energy required for the process. As the price of minerals and metalliferous ores and the efficiency of microwave processing technology increase, one might predict that this will soon be the case.

In the case of concrete waste, one could argue that the development of a microwave-based recycling process has perhaps even more potential than with mineral beneficiation. Some arguments to this effect include:

- Recycling concrete has the potential of eliminating a waste stream altogether by recycling all its constituents. Being a high-value man-made material with significant energy and material footprint, the recycling of concrete is a priority.
- Recycled cement can re-enter the clinker-making process (Costes et al., 2010) and thereby contribute to reducing the CO_2 emissions of clinker production by direct substitution with natural carbonates. Reusing cement will also contribute to preserving natural carbonate reserves. Also, the presence of already decarbonated and crystallised phases in recycled cement may also have a positive effect on the energy balance for making clinker, through a possibly reduced heat requirement due to the reduced initial mass and lower required temperatures.
- Recycled aggregate can re-enter the concrete-making process and contribute to preserving natural aggregate resources, which is becoming a scarce resource in developed countries, particularly when dealing with aggregates of alluvionary origin.
- The proximity of concrete waste to consumption areas may contribute to reducing transport associated with the concrete-making industry.

The sensitivity of concrete to microwaves has been known for some time. Using a 5-kW multimode microwave oven and exposure times up to 30 minutes, the possibility of liberating aggregates from hardened cement for concrete analysis purposes was tested over 30 years ago by Figg (Figg, 1974). His pioneering work with 100-mm cubes brought convincing evidence that microwaves could indeed induce boundary fracture at the aggregate-cement interface. At high power inputs, concrete has also been shown to respond explosively, with commercial applications in drilling (Jerby at al., 2002) and controlled spalling (White et al., 1995).

The application of microwave-heating to the issue of concrete recycling is a relatively new endeavour, but one that has already been shown to be effective. Akbarnezhad and co-workers (Akbarnezhad et al., 2011), using a 10-kW generator, showed microwave heating prior to physical comminution to improve recycled aggregate properties, and that this effect is superior to comparable techniques using purely mechanical means or a combination of mechanical means and conventional (external) heating. About the same time, the authors (Lippiatt and Bourgeois, 2012) showed that microwave heating of concrete increases the liberation of aggregate and cement, while decreasing the strength of concrete.

Eventually, impact breakage of these microwave-heated particles of concrete was carried out using a short Hopkinson bar (Bourgeois and Banini, 2002). Liberation was measured using a dissolution technique based on the work of Kiss and Schönert (Kiss and Shönert, 1980).

The results of this previous work validated the hypothesis that the microwave heating of concrete, followed by impact breakage, improves aggregate liberation, thereby opening avenues for recycling concrete. Moreover, the degree of liberation was found to increase non-linearly with exposure time, hence input microwave energy. The short and medium exposures did lead to a similar level of aggregate liberation, which exhibited a significant increase after the long exposure.

Cement liberation was not measured directly but by the mass lost during dissolution. Cement distributions were nearly the same for samples that had undergone short and medium microwave exposures, and cement fines increased dramatically with the longest treatment. It is noted that the sharp increase of cement liberation with the long exposure to microwaves, followed by impact breakage, mirrors the increase in liberation of aggregates by the same process.

Analysis of Hopkinson bar impact tests revealed both a reduction in impact fracture force with increasing exposure, and a progressive loss of elasticity of the concrete with the mechanical behaviour of the most damaged samples resembling that of a loose-packed bed.

These quantitative observations are conclusive indicators of the value of microwave heating for recycling concrete. In summary, when followed by impact breakage, the microwave heating of concrete increases aggregate liberation, increases cement fines and reduces concrete strength.

However, the macroscopic nature of these observations, which result from the combined effect of microwave heating and impact breakage, does not permit understanding what is actually happening inside concrete during microwave heating. The authors argue that some understanding about the microstructural changes that occur at the local scale inside concrete during microwave heating is essential for defining the scope and place of microwave heating in a concrete recycling process. The ultimate goal that this paper aims to move towards is to precisely unravel the elements of reconciliation between variations at the microscopic and macroscopic scales, so as to provide guidelines for the development of an efficient concrete recycling process.

2. Materials and methods

Our ability to relate observations between both scales requires that we quantify the textural changes that take

place inside concrete during microwave heating, especially near the aggregate-cement interface and inside the cement matrix itself. In the process of developing a satisfactory texture analysis protocol, several experiments were performed. This preliminary work led to some appreciation of what had to be quantified for the sake of understanding the link between changes in the microstructure and macroscopic behaviour of concrete. It was concluded that microstructure quantification would have to focus on the properties of cracks, whose patterns were found to change most significantly during microwave heating. Mineralogical changes, as measured by X-ray diffractometry, did not reveal significant changes in comparison. Having decided that the formation of cracks should be the focal point, efforts were allocated during this work to establishing an experimental protocol that would not alter the fractures caused by microwave heating. A non-destructive observation protocol using the scanning electron microscope for texture image acquisition was designed for this very purpose, avoiding altogether any requirement for crack impregnation, cutting or polishing after microwave treatment of the concrete samples.

2.1 Concrete sample preparation

The concrete used in this work was made with cement-enriched mixture (CEM) 1 52.5 Portland cement. Samples were mixed in five different ratios (See **Table 1**) with siliceous aggregate 2–2.5 mm in size. The sample preparation protocol is schematised in **Fig. 1**. Samples were cast in 20-mm cylinders, which after curing, would weigh about 10 g each. After setting in the mould for 24 hours they were removed and allowed to cure in water at room temperature for a minimum of 90 days.

The samples were then removed from soak and separated into lots of 12 units. One sample was reserved for mercury porosimetry analysis, ten for Hopkinson bar impact testing, and one was cut using a water-lubricated diamond saw to give an exposed cross-section. The purpose of this operation was to create a flat surface that could be readily observed after microwave treatment, without requiring any post-treatment cutting or polishing that could potentially alter the fractures induced by the heating process. An alternative would have been to impregnate uncut samples after microwave treatment with a polymer resin or Wood's metal, and then cut and polish to expose an observable flat surface. However, this approach was rejected outright for it had the potential to damage the fractured microstructure. One downside of the protocol that was adopted here over the alternative was that it made the observation of fractures possibly more difficult due to the lack of contrast of the fractures against

Table 1 Properties of concrete samples

Concrete samples	Water/Cement mass ratio	Aggregate/ Cement mass ratio
S1	0.4	0.6
S2	0.4	0.85
S3	0.4	1.6
S4	0.5	1.6
S5	0.6	1.6

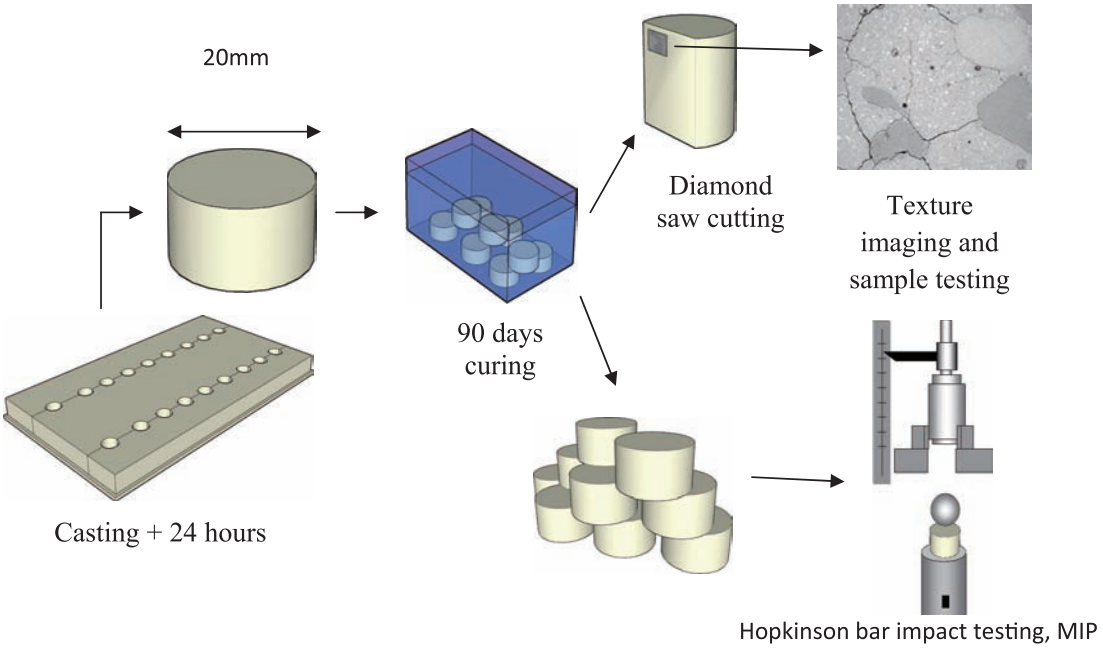

Fig. 1 Illustration of the concrete sample preparation protocol.

the solid phases. This was found to be a problem particularly with untreated samples. The measurement is based on a subjective judgement of contrast and shape. Untreated images showed even less contrast than treated samples.

Some might consider ten samples an insufficient number of samples for mechanical tests of this type. At this stage, the goal is merely to seek patterns so that more extensive testing and results distribution analysis is unnecessary. All results are presented with the mean and full range of measured values.

Prior to testing, samples were systematically dried at 50°C for 24 hours before any microwave treatment or analysis began so that all samples would be equally dry before testing. This was validated by measuring the sample mass changes with drying. After 24 hours at 50°C, the samples stopped losing mass at room temperature.

2.2 Microwave testing and sample post-treatment

Higher power densities are more effective in embrittling multiphase materials (Ali, 2010) and the highest power densities are produced in single-mode cavities (Kingman et al., 2004b). The samples were heat-treated in a 2-kW/2.45-GHz single-mode horizontal waveguide applicator designed by SAIREM. The samples were heated in the microwave system individually; the sample moulds were designed so as to make use of the 30-mm microwave transparent, cylindrical, silica sample holders. The position for the iris and the short circuit for minimum reflected energy were found manually. The iris position was kept constant for all tests. If the initial reflected energy was higher than expected, the short circuit was moved to accommodate. This change in position was never more than a few millimetres.

The samples were treated for 3 characteristic times and the power absorption signal was recorded. These times are seen in **Fig. 2**, and correspond to 15, 30 and 50 seconds called 'short', 'medium' and 'long' treatment, respectively. Short, medium and long microwave exposures are annotated as 'S', 'M' and 'L' so that S1-0, S1-S, S1-M and S1-L represent untreated, short, medium and long treatment times of concrete sample S1, respectively.

They were chosen as they were found to represent three distinctly different stages in the microwave heating cycle for the cast concrete samples under the conditions of the test. The 'short' time comes just after the initial absorption peak, during which 50 to 70% of the sample mass loss occurs, as water evaporates readily. The 'long' time occurs before the absorption starts to peak again, and the 'medium' time corresponds to an intermediate time between these two events. The formation of this microwave absorption peak usually occurred after approximately 50 seconds but was not totally predictable. It is assumed to occur after the formation of local thermal runway and consequently the formation of a plasma. Although the reflected power was measured in real time, the microwave cavity is an open system that can lose mass and energy by convection and evaporation, so the measured energy and power absorbed by each sample is only a guide, and cannot be used as absolute energy absorption by the samples.

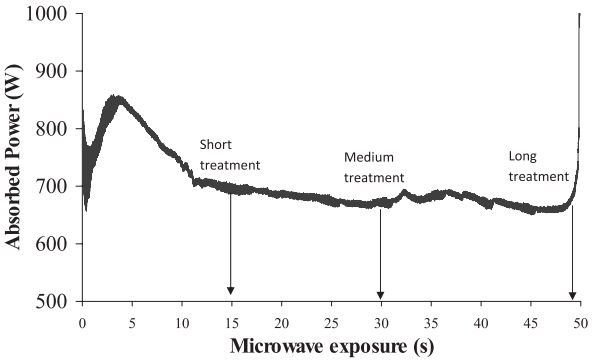

Fig. 2 Typical microwave power absorption record for a 20-mm cylindrical concrete sample (S1).

After cutting the power at the end of the test, an estimate of the average temperature reached by a sample was obtained using a Jules Richards Instruments Flashpoint FX400 infrared thermometer pointed at the sample surface. The temperature was measured on each of the sample's three surfaces. The mean of the highest recorded temperatures of each sample was recorded as the temperature achieved after treatment. Due to conduction with the experimental surface between measurements, the highest temperature measured was usually the first temperature measured. The maximum temperature was chosen as the representative temperature because of the temperatures measured, it exhibited the least variation. The four surfaces of cut samples were also measured but these values were not used in the temperature calculation due to the difference in sample mass. The samples were weighed individually prior to and after microwave treatment, in order to record the mass loss associated with the heating process. Initially, they all weighed about 10 g.

Eventually, a number of tests were systematically performed on the samples. These measurements included:

– Total porosity and pore size distribution by mercury intrusion porosimetry. This was performed using standard 400 MPa intrusion with a Micromeritics Autopore IV.
– Impact breakage testing using a vertical Hopkinson bar. The cylindrical steel bar used was 40 mm in diameter and 1.5 m long. The impactor was a 60-mm diameter, 825-g steel ball bearing dropped from a height of 163 mm and 200 mm. In previous work, a drop height of 163 mm was found to be the minimum required to break an untreated 20-mm concrete cylinder so it was used again for consistency. The 200-mm drop was used

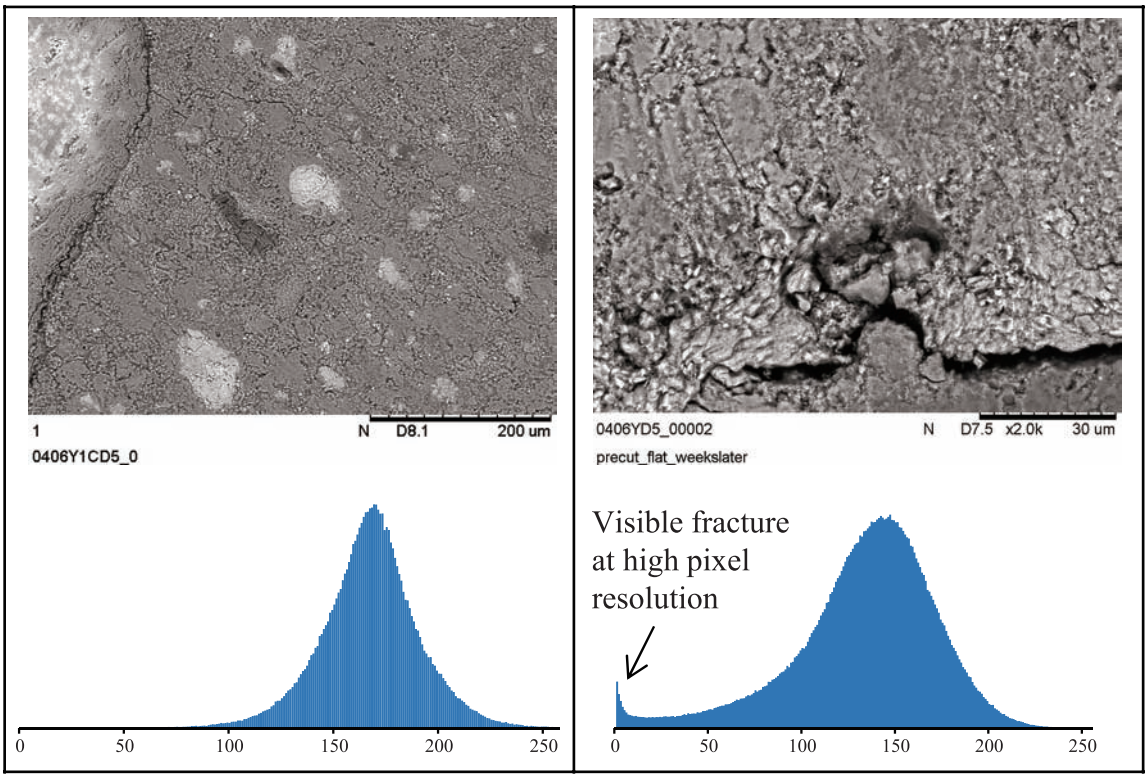

Fig. 3 Standard intensity histogram for SEM images of S1-0 sample. Left: 400× magnification = 0.9 μm/pixel, right 2000× magnification = 0.2 μm/pixel.

to decrease the number of unbroken samples. This does not affect the measure of force required to fracture a sample unless a sample is sufficiently damaged that it no longer displays brittle elastic fracture properties.

– Capture of flat surface images using a Hitachi TM3000 Tabletop Microscope SEM, at different resolutions. The following section is dedicated to this specific part of the sample analysis protocol, which deals with measuring the local effect of microwave heating on the concrete texture.

2.3 Acquisition and analysis of concrete texture images

As indicated previously, the flat surface of the concrete samples, whether treated or untreated, was observed as is by SEM, i.e. without any post-treatment tampering. The SEM images were obtained in this work using a Hitachi TM3000 set to an acceleration voltage of 15 kV. Image analysis of electron microscope images have already been used with success in concrete and cement analysis (Ben Haha et al., 2007; Igarashi et al., 2004; Wong et al., 2006). For the sake of analysing the fractures transecting the flat surface of the concrete samples, the use of SEM images proved to be rather challenging. Indeed the grey-scale intensity of SEM images shows significant overlap between the fractures and the solid phases. **Fig. 3** shows that almost every phase present is included in the same grey level peak.

Given the significant overlap in grey-scale intensity, the binarisation of images is difficult to automate. By careful preparation and observation of samples under sufficiently high magnification, as per the image on the right of **Fig. 3**, the intensity histogram can be separated sufficiently into different peaks so that automated image analysis can be performed on SEM images of concrete and other cement-based materials (Brough and Atkinson, 2000; Yang and Buenfeld, 2001). Examining larger objects such as aggregate particles and the fracture growth that occurs around them requires a lower magnification, meaning greater sample surface area in an image, for reasons of representativity. This lower zoom level has the side effect of condensing the grey-level histogram, making automated image analysis more difficult. Even when highlighted manually, there is the fear that fractures are mislabelled due to low contrast. By repeating the liberation measurement on 40× (9 μm per pixel) images, the uncertainty in the liberation measure was estimated to be no greater than 5% total interface length.

The fractures observed in this work are spaced at distances such that if images were taken at high magnification, say 2000×, then it was very easy to take an image that showed no fracture, even when the sample was highly fractured. When using a low magnification, say 50×, although the high area covered by an image meant the

image was more representative of the sample, it also meant that smaller cracks that were visible at higher magnifications would not be included in the analysis. The minimum zoom possible on the SEM equipment used is 40×, which corresponds to a pixel resolution of 9 μm per pixel. For this work, two zoom levels were chosen, 40× and 200×. Images taken at 40× zoom were chosen to measure the liberation of aggregates as, after cursory examination, a large apparent variation was observed between aggregate particles and this zoom level allowed the largest possible fraction of a sample to be investigated. Another set of images was taken at a zoom level of 200× so that crack networks not visible at a larger scale could be investigated. The number of images was chosen in such a way as to yield a satisfactory compromise between representativity (giving a stable average of textural properties) and keeping the number of images to a minimum, given the strain of the manual digitisation work involved. A scaled comparison of the size of images taken at different SEM magnification levels is shown in **Fig. 4**.

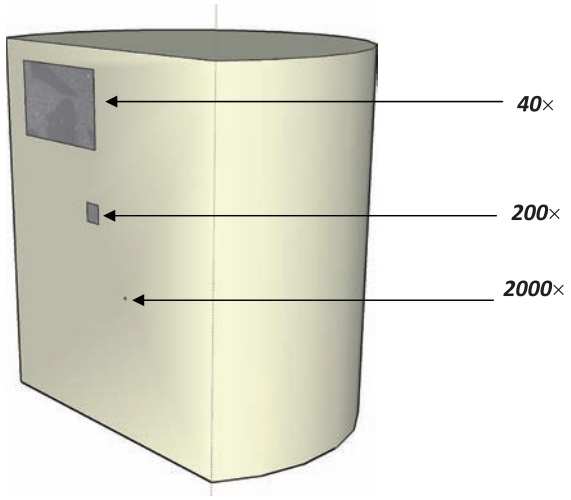

Fig. 4 Comparison of area covered at different zoom levels on sample cut surface.

To overcome the lack of contrast, sample images were highlighted manually. This technique, despite its tediousness, presents a satisfactory way to deal with the aggregate/cement contrast overlap simultaneously with the porosity/fracture contrast overlap. Although the technique has been rightfully identified as imperfect, it has also been used to justify the accuracy of automated image analysis methods (Brough and Atkinson, 2000). In this case, if one of the techniques is accurate, then both must be. **Fig. 5** shows an SEM image before and after highlighting. Aggregates and fractures are easily recognisable. The meaning of the colour-coding of the highlighted image fractures is explained later.

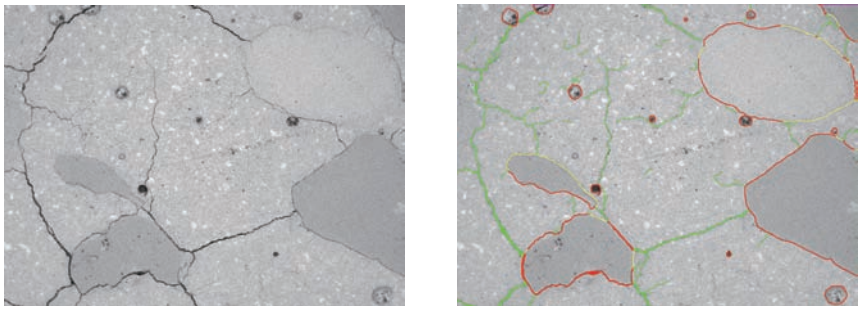

Fig. 5 Example of original and highlighted images taken at 40× zoom for an S1-M sample.

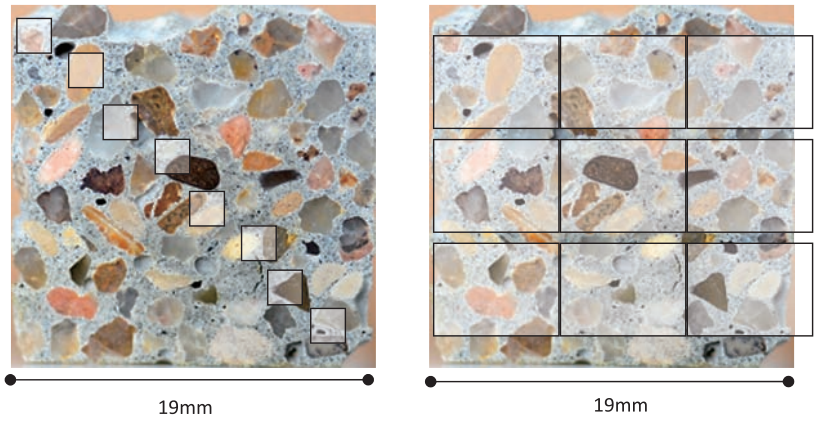

Fig. 6 Illustration of the concrete SEM imaging scheme. Left: images sampled at 200× magnification, Right: images sampled at 40× magnification.

Quantification of fractures being the focal point of the analysis of concrete microstructure after microwave heating, a number of properties were used to quantify fracture porosity.

Straightforward variables that can be measured are the length of, number of and width of cracks present in a given sample area. For the purpose of quantitative image analysis, it was decided to capture 10 SEM images for every sample, 480 pixels by 640 pixels in size, at 9 μm per pixel (40× magnification) and at 1.8 μm per pixel (200× magnification). **Fig. 6** shows the scale and positions of the 10 non-overlapping images for both resolution settings, relative to the 20 mm concrete sample.

Fractures were highlighted manually using a Wacom DTU-2231 interactive pen display. One advantage of this manual image analysis scheme is that it permitted careful hand delineation of different components present in the images, thereby differentiating different classes of fractures. The key highlighted components were:

- Aggregate/cement interface with fracture
- Aggregate/cement interface without fracture
- Fractures within the cement bulk
- Fractures within aggregate particles

As illustrated in **Fig. 7**, every component of interest to the work was highlighted using a distinct colour, which could eventually be used for counting purposes. Six colours, easily distinguished in RGB format, were used (pure green, pure blue, pure red, pure green/red-yellow, pure blue/red-magenta, pure green/blue-cyan), seven including the areas not highlighted (the entire grey-scale from black to white).

Having highlighted different components of interest with distinct colours, a number of insightful quantitative properties, which will be eventually tied to macroscopic variations in concrete properties and operating conditions, could be easily post-treated. They included the properties of fracture per se, as well as the properties that were deemed directly relevant to processing performance.

Starting with the former, the total crack length was measured from skeletonised highlighted images, whereas the total area of cracks, both in the cement bulk and between aggregate and cement paste, and average crack width were measured directly from the highlighted images.

In some images, it is sometimes difficult to tell the difference between a large pore that has formed from an air pocket and one that is the result of an aggregate that is no longer present. Both have a similar shape and appeared to have a similar effect on fracture growth. For initial analysis, all such objects were marked as liberated aggregate. This decision was made to reduce the subjectivity in the analysis process. A side effect of this decision is that all textural liberation values are overestimated. Re-analysis of the S1-0 samples places this variation no greater than 10% of the total aggregate interface length. As all samples were made in the same manner, it can be assumed that the quantity of such large pores is common between samples. Such a systematic error can be ignored in that its biasing the actual values does not change the comparative analyses and conclusions drawn.

Looking now at properties that relate directly to processing performance, the textural liberation of aggregates

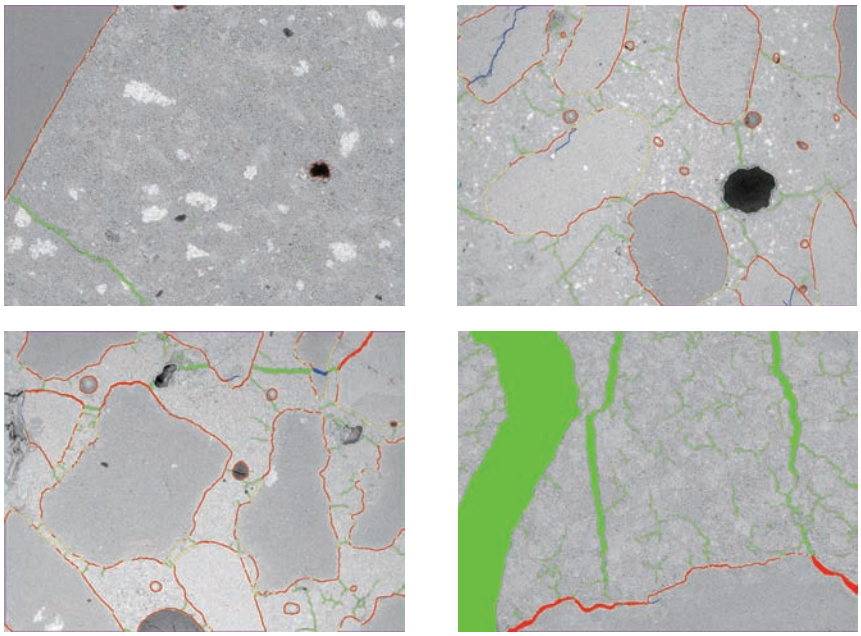

Fig. 7 Examples of highlighted SEM images. Clockwise from top left: S1-0 at 200× zoom, S1-S at 40× zoom, S3-L at 200× zoom, S4-M at 40× zoom.

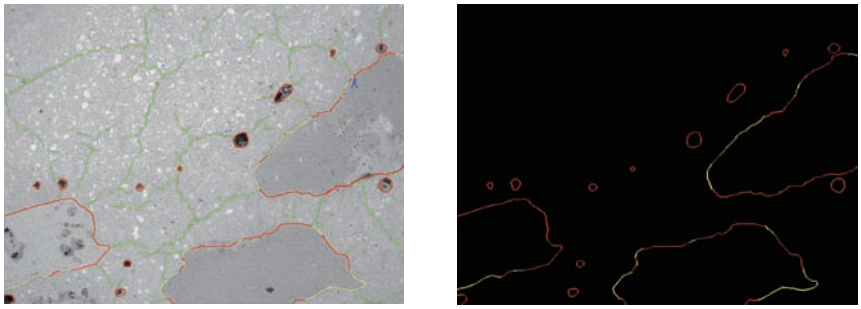

Fig. 8 Example of aggregate textural liberation measurement, S1-M at 40× zoom.

was defined as the ratio between the fractured and total aggregate boundary lengths. **Fig. 8** shows an image with a textural liberation value of 76%.

Aggregate liberation was measured using the 40× zoom (9 µm per pixel) images for the sake of representativeness. The cracks in the cement paste, however, were significantly finer, and were observed using 200× zoom (1.8 µm per pixel) images. During analyses it was found that there appeared to be two different types of fractures forming within the microwave-treated concrete samples. The first group formed the 'primary network', and included all the fractures at the interface of an aggregate particle and the cement paste and all fractures that branched from this interface. This network was visually identified as being made of a few large fractures which ran from aggregate to aggregate throughout the sample. The second group formed the 'secondary network', and included a large number of smaller fractures that spread throughout the cement phase. **Fig. 10** illustrates the 2 families of fractures, which were assigned different colours for quantification purposes. Aggregate fractures occurred also, especially in long-treated samples. However, aggregate fractures occurred to a far lesser extent than cement and grain boundary fractures so were not accounted for in the analysis, which allowed one of the nine colours to be re-assigned so as to permit differentiation between primary- and secondary-network cement paste fractures. In **Fig. 9** and **Fig. 10**, primary network fractures are displayed in yellow.

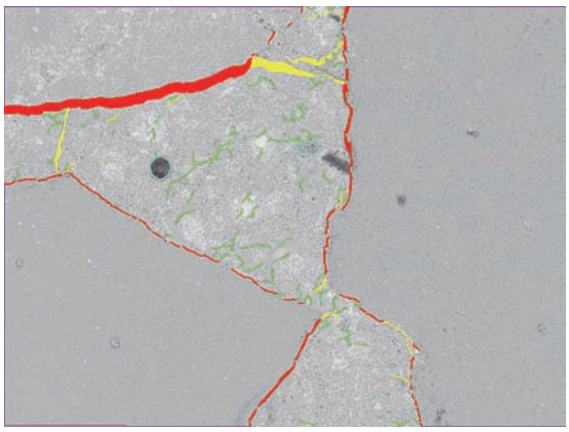

Fig. 9 Example of primary and secondary fracture network highlighting.

Once the images were skeletonised and fractures sorted into primary and secondary networks, the nodes and ends of fracture branches were then counted automatically. A branch is defined as a length of fracture between nodes and/or fracture ends.

Because the post-treatment of highlighted images is

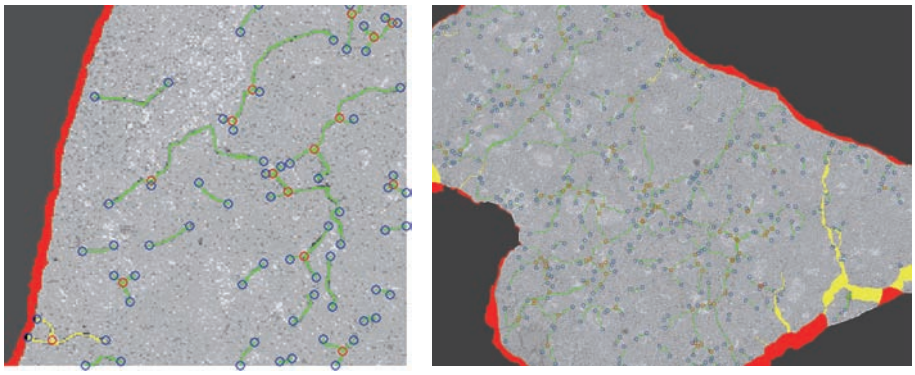

Fig. 10 Example of identification of branches and nodes in the secondary network of fractures. Yellow: primary-network-cement paste fracture, green: secondary-network fracture, red: aggregate/cement interface fracture-primary network, red circle: node, blue circle: branch end.

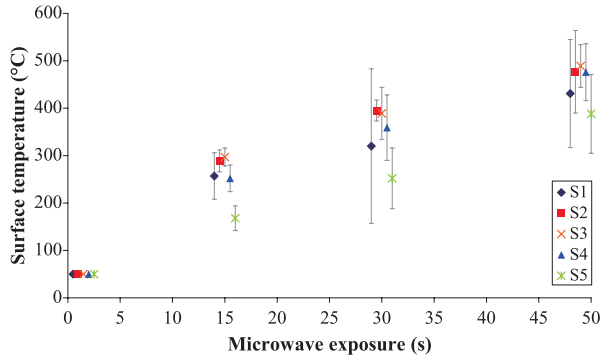

Fig. 11 Measurement of surface temperature as a function of test duration (exposure time offset for clarity).

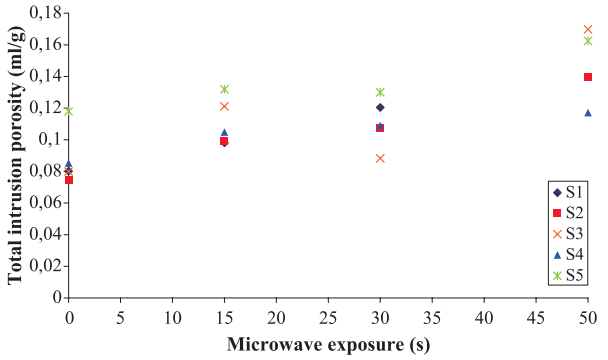

Fig. 13 MIP measurement of total sample porosity for S1 to S5 concrete samples.

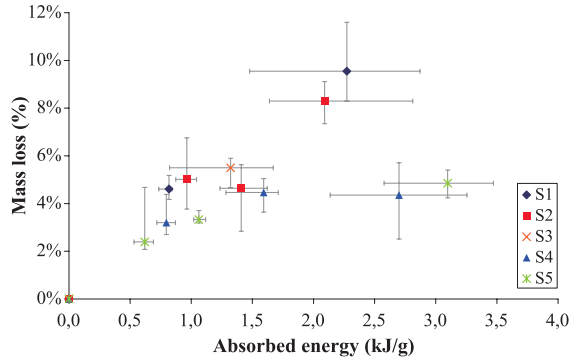

Fig. 12 Correlation between mass loss and energy absorption.

automated, some fractures will necessarily be misclassified, as for example some primary fractures will be connected to aggregates that are not contained in the image, or a primary fracture will branch into two almost identical branches. However, such occurrences are rather rare and do not change the value of the results obtained considering the large number of fractures.

3. Effect of microwave heating on concrete: macroscopic level results and analysis

This section presents the results of measurements made on concrete samples at a macro scale. It shows the temperature, mass loss, fracture strength and the MIP (mercury intrusion porosimetry) porosity changes associated with microwave treatment in different concrete samples. This macroscopic level analysis is used to justify the necessity for local, textural analysis of the effect of microwave heating on concrete.

Microwave treatment increases the temperature of concrete samples, albeit in a different way to that of conventional heating as external heating conducts from the sample surface, whereas microwave heating occurs within the sample. Nevertheless, the longer the application of microwave power, as shown in **Fig. 11**, the greater the temperature measured at the surface of the concrete samples. Despite the S5 sample exhibiting a slightly different trend, it is fair to say that the elevation of temperature, as measured at the samples' surface, is comparable for all concrete sample types tested with short, medium and long treatments.

With the samples tested, it can be concluded that the average temperature reached by the samples does not depend significantly on the variations in concrete properties, at least within the variable range represented in samples S1 to S5 (See **Table 1**). As can be seen in **Fig. 11**, the amount of energy absorbed by each sample is nearly proportional to time once the initial water absorption peak is over. The power input was set to the same 2 kW nominal value for each test. This implies that the differences in thermal properties, dielectric properties and mass compensate for each other and/or they are insignificant in the range tested. As will be seen later, differences in textural properties within the samples are also marginal, suggesting that microwave heating of concrete exhibits a low sensitivity to concrete properties. This is a valuable result from a recycling standpoint as it suggests a concrete recycling process will be insensitive to input properties and no special expense or effort is necessary to accommodate varying concrete waste streams.

The energy absorption by the concrete samples is strongly correlated with the mass loss, as shown in **Fig. 12**, which is itself caused by water loss during heating. It is possible that mass other than water can be lost, however, this effect is deemed insignificant and so all mass changes can be safely assumed to be due to the loss of water. It is also noted that X-ray diffraction spectra did not show any noticeable mineralogical changes between treated and untreated samples, confirming that decomposition of crystallised phases such as portlandite and calcite are marginal at best at such temperatures (Piasta et al., 1984).

By means of MIP, the changes in porosity were characterized with all 5 samples under their untreated and

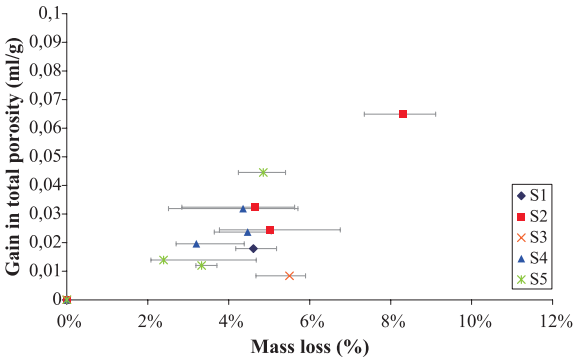

Fig. 14 MIP measurement of total sample porosity as a function of mass loss.

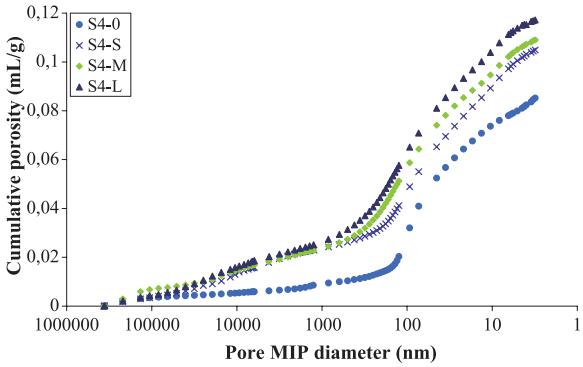

Fig. 15 Measurement of pore size distribution using MIP for sample S4.

microwave-heated states. **Fig. 13** shows the total intrusion porosity, a measure of the total volume of pores in the samples. The data is given on a sample mass basis. There is a consistent increase in total porosity with increased energy input into the concrete samples, for all concrete samples tested.

Although water loss plays a significant role in the porosity gain, as would naturally be expected, **Fig. 14** shows that there is no clear trend between the measured increase in sample porosity and the actual mass loss.

Assuming MIP accurately measures the total porosity, converting the mass loss from **Fig. 14** into the equivalent volume of liquid water shows that bulk water loss could not explain more than 60% of the pore volume that is created. Water loss must come from sources other than free water, such as the decomposition of portlandite and hydrated calcium-silicate (CSH).

This simple calculation indicates that more than 40% of the total porosity created and measured by MIP is associated with mechanisms other than bulk water loss during the exposure of concrete to microwave heating. This trivial analysis illustrates further the intrinsic complexity of porosity changes during the microwave heating of concrete, making a compelling argument for investigation of porosity changes at the local scale, by direct observation of concrete texture.

Fig. 14 seems also to indicate that the higher the water to cement ratio (w/c), the lower the contribution of water loss to the increase in total porosity. This observation indicates that whatever phenomenon other than bulk water loss is causing an increase in microwave-heated concrete porosity, it is associated with the w/c ratio and its effect on concrete microstructure, i.e. porosity. A more porous concrete sample is more prone to evaporation during microwave heating. If we assume the samples made with a higher w/c ratio had less water in their pores (relative to saturation) before treatment, then it makes sense that the evaporation of this type of water contributed less to pore formation. It is also logical that these concretes were more susceptible to other crack formation mechanisms related to drying as they would dry faster and thus be affected by these mechanisms sooner. The results also suggest that there is no significant pore growth due to excessive pore pressure as this would presumably occur more in the lower w/c ratio samples due to their smaller pore volumes. This does not mean that this phenomenon does not contribute significantly to mechanical changes or aggregate liberation. The explosive spalling of some low a/c samples in the first 5 seconds or so of microwave treatment (~100°C) might suggest this is an important phenomenon in terms of concrete recycling, but it does not appear to be an important phenomenon in increasing sample pore volume.

Despite its limitations, the pore size distribution measured by MIP can give some appreciation of the evolution of porosity within concrete samples with microwave heating. One example is given in **Fig. 15** for concrete sample S4. Bearing in mind the limitations of MIP measurement, namely its sensitivity to the ink-bottle effect (Diamond, 2000), what the measurements confirm is that a connected network of large pores, measured to be in the 1–100-μm range, exists in all microwave-treated samples. MIP does not measure this network in the untreated samples. This behaviour was consistently found with all concrete samples tested. One possible explanation is that the connected pores created by a short exposure are becoming larger as a result of heat-induced shrinkage of the cement phase. An interesting observation is that MIP does not appear to see noticeable changes below the 1-μm range between short and long exposure.

Along with changes in porosity, concrete performance is altered in a dramatic way by microwave heating. As reviewed earlier in the paper, the liberation of aggregate and cement was found to increase with exposure to microwaves. Analysis of microwave-heated samples using the Hopkinson bar also revealed strong changes in mechanical properties. **Fig. 16** shows the change in fracture force for the 5 samples considered in this paper, as an illustration of the embrittlement caused by microwave heating. Fracture

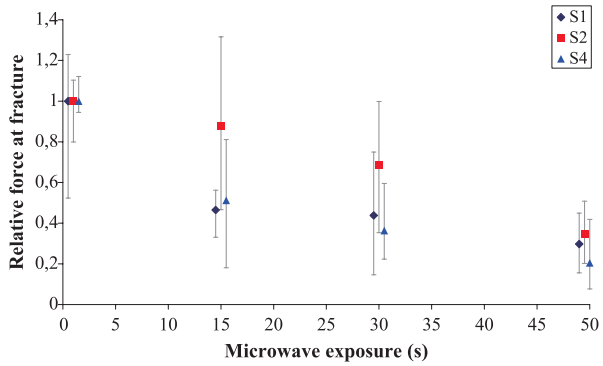

Fig. 16 Hopkinson bar measurements of impact fracture force on microwave-heated concrete samples (exposure time offset for clarity).

force is normalized by the fracture force for the untreated sample, which takes value 100%. This allows a simple assessment of the relative change in fracture force as a function of microwave exposure.

It is consistently found that the relative fracture force decreases continuously with increased exposure to microwaves, possibly with the largest loss in mechanical properties occurring after the short exposure. These are interesting observations, particularly in light of the knowledge that aggregate and cement liberation increases most significantly after a long exposure to microwaves, as seen earlier in **Figs. 1** and **2**. These observations suggest that there is some embrittlement phenomenon that is not effectively observed when using macro-scale measurement techniques, and there is not a direct link between changes in mechanical behaviour and physical liberation.

Overall, the macroscopic analysis has provided us with interesting insights about the changes that occur inside concrete during microwave heating, causing a change in mechanical behaviour, with a loss of resistance to impact fracture that varies continuously with increased exposure, and an increase in liberation of both aggregate and cement phases, albeit significant for the long exposure only. The main change related to concrete microstructure is associated with porosity, which increases continuously with exposure, as seen from both total porosity and pore size distribution measured by MIP. The changes in mechanical behaviour seem to vary as per the changes in total porosity, and a link between porosity and physical liberation of aggregates can be inferred.

The disparity between the evolution of physical liberation and mechanical properties with microwave exposure illustrates the need to further understand the microwave-heating concrete-embrittlement mechanisms with a local technique. For this work, image analysis of SEM images was chosen.

4. Effect of microwave heating on concrete: local level results and analysis

As discussed in the preceding section, the changes in porosity that occur during microwave heating of concrete are possibly numerous and complex, making the observation of porosity at the textural scale a compelling step towards unravelling the mechanisms by which microwave heating alters concrete. As will be shown here, textural analysis of the structure of fracture porosity provides an insightful angle on the mechanisms that take place inside concrete as it is being heated by microwaves, with views on recycling its elementary constituents.

Fig. 17 shows a superimposition of some highlighted images of sample S1. It is noted that the same general pattern applies to all the concrete samples tested in this work, with differences in the magnitude of the observed changes. Looking at the obvious changes in fracture porosity between the images, **Fig. 17** also validates the authors' selection of the 4 characteristic times along the heating process for the sake of quantifying the effect of microwave heating on concrete texture.

- Untreated concrete samples exhibit only few fractures, at both 40× and 200× magnification. Fractures are essentially found around the aggregates, in the region known as the interfacial transition zone (ITZ).
- After the short treatment, the sample having been heated for 15 seconds, a large-scale network of fractures appears, visible with the 40× magnification. These fractures seem to form a network connecting aggregate particles and also appear to run around them, going through the entire sample texture. This network is referred to as the "primary fracture network". As it is associated with aggregate grain boundaries, the formation of this network is directly associated with the liberation of aggregates.
- When the concrete sample is further heated to the medium condition (30 seconds), fractures from the primary network widen. Another network of smaller fractures develops that invades the cement paste. Because it appears to be nested within, and is of a smaller scale than the primary network of fractures, it is referred to as the "secondary fracture network".
- At the long exposure (50 seconds), while the primary network keeps widening, the quantity and length of the secondary network fractures increases significantly.

These generic observations are visible with every tested sample to a varying extent. From a range of observations that were repeatedly made during this study, it was ascertained that a strong correlation exists between the properties associated with the primary network and the loss of mechanical strength and liberation of aggregate particles. The properties of the secondary network further explain the mechanical changes but more importantly provide the

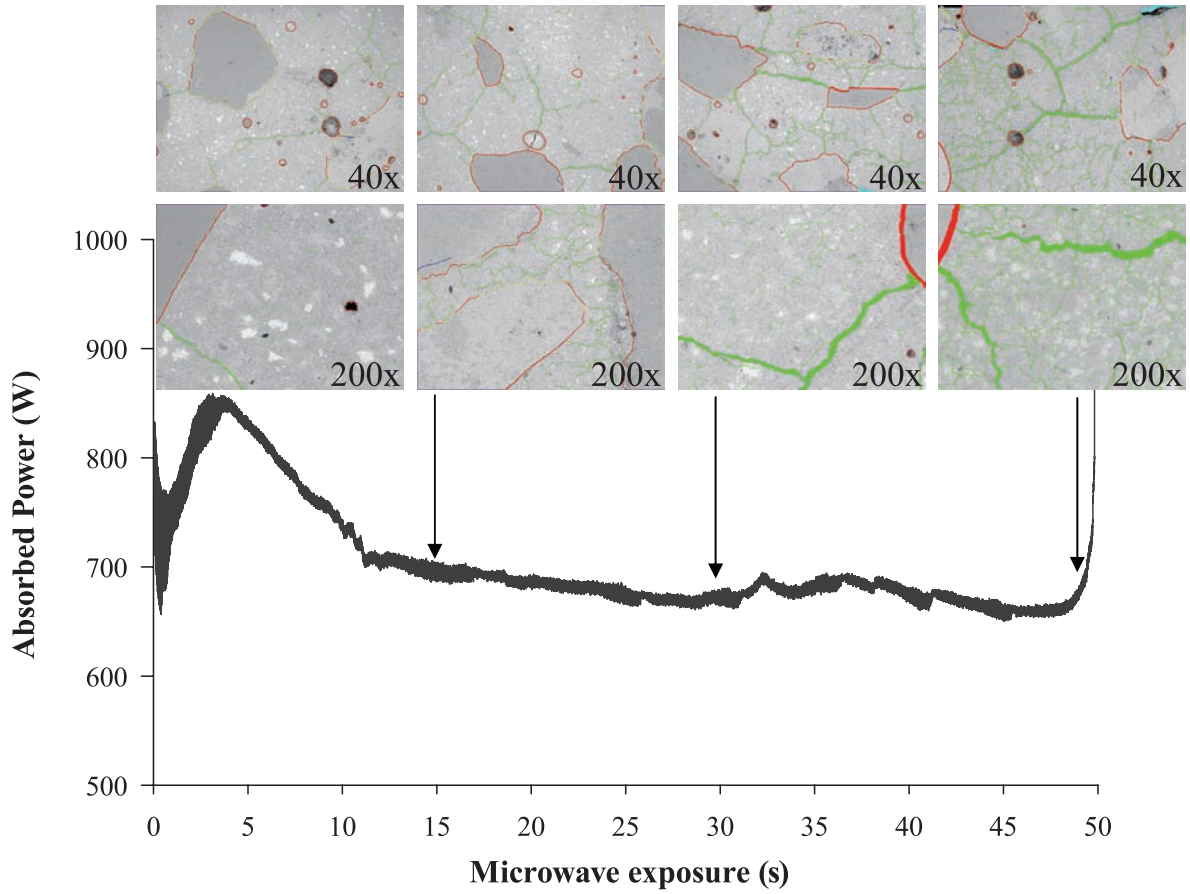

Fig. 17 Local observation of porosity changes with microwave treatment of S1.

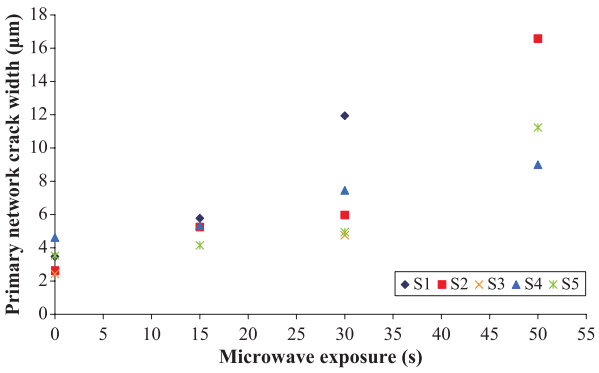

Fig. 18 Variations in primary network fracture width with microwave treatment time.

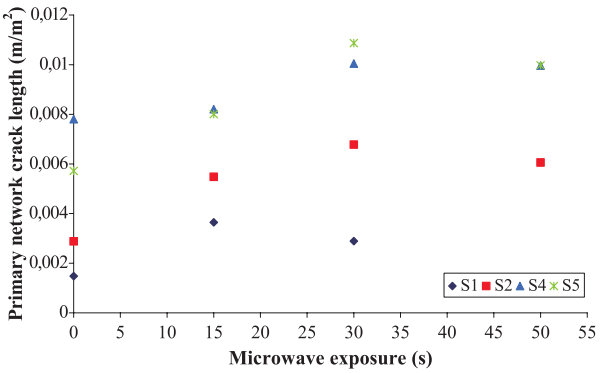

Fig. 19 Variations in primary network length with microwave treatment time.

link between textural liberation and physical liberation, as measured by impact testing, specifically the fineness of the cement paste fragments after impact testing.

Because these networks correlate directly with the macroscopic properties of microwave-heated concrete samples discussed in the previous section, their formation and growth are thought to hold the key to concrete recycling. The following section is concerned with quantification of both primary and secondary fracture networks.

4.1 The primary fracture network

The primary network may be quantified in a number of ways. Accessible properties from two-dimensional images include average properties such as total length, surface area and crack branch number, and statistical properties such as crack branch length and size distributions. As seen in **Fig. 18**, the width of primary network cracks increases very rapidly with microwave exposure. Conversely, as seen in **Fig. 19**, once the network is formed after a short

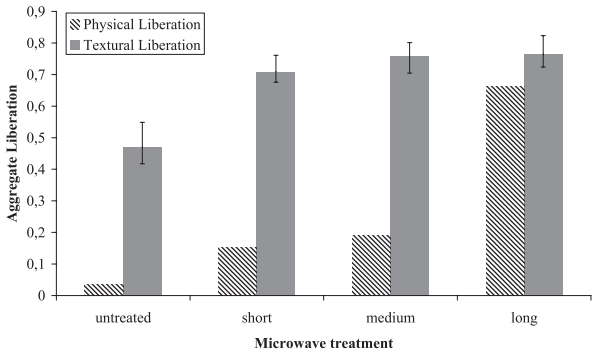

Fig. 20 Comparison between physical liberation (Lippiatt and Bourgeois, 2012) and textural liberation of aggregate particles.

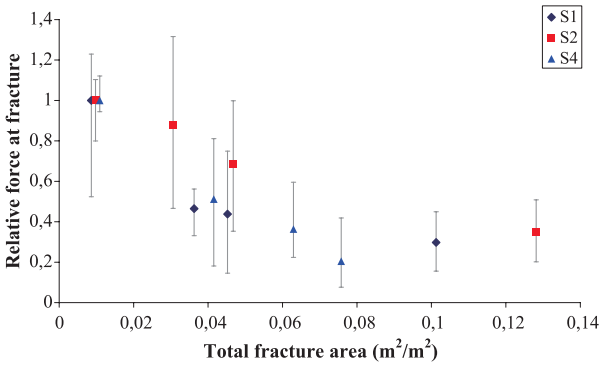

Fig. 21 Relative change in concrete strength, as measured by the relative force at fracture as a function of the combined area of primary and secondary networks relative to the cement paste area.

exposure, the length of the primary network is relatively unchanged. What this indicates is that the fractures that form this network widen with increased exposure, but do not propagate significantly beyond the extent reached after a short exposure to microwaves. The mechanisms associated with the change in thickness of primary-network fractures are deemed to be associated with drying shrinkage of the cement matrix. Because of the specific properties of the ITZ with its high porosity, micro-fracturing and water content (Roy and Idorn, 1993), a strong local reaction to microwave heating is bound to occur around the ITZ during microwave heating, and the formation and growth of the primary fracture network is expected.

By definition, the primary network is associated with what was earlier defined as the textural liberation, which accounts for the fraction of the aggregate perimeter that is liberated in the 2D analysis. **Fig. 20** compares physical liberation, as measured by acid dissolution, with textural liberation. Because the work presented here spans a long period of time, these measurements were not made on the same samples, hence changes in sample properties may contribute marginally to the observed differences. The error bars represent the range of textural liberation values from all the tested samples, the height of the bar representing the average value. The physical liberation values were measured on 10 mm cubes (Lippiatt and Bourgeois, 2012).

Textural liberation is already significant with the untreated sample. The high porosity of the ITZ, often with extensive micro-fracturing, is well documented (Roy and Idorn, 1993). Using MIP, Roy and Idorn estimated values of porosity in the ITZ as high as 37%. Mehta and Monteiro (Mehta and Monteiro, 2005) predict a high level of aggregate boundary fracturing from drying shrinkage during concrete heating, hence the observation of the primary network formation during microwave heating is expected.

Fig. 20 shows that textural liberation reaches a very high value after the shortest of the three measured microwave exposures, and it does not increase significantly after that. Aggregates are highly liberated inside the concrete texture after a short exposure to microwaves only. This is an important piece of information from a processing standpoint, as an increased duration of microwave heating becomes directly an increase in energy consumption. Nevertheless, upon impact breakage testing, the aggregate particles remain trapped inside the cement matrix. Indeed, the 2D analysis finds 70% of the aggregate boundaries being liberated in the concrete sample for the short exposure, when only 15% of the aggregate is physically liberated after single-particle impact breakage of a short-treated sample. It is fair to conclude that single-particle impact breakage cannot harvest the liberation induced by microwave heating. In other words, an alternate form of comminution is required to take advantage of the textural liberation of aggregate particles.

Eventually, for the long exposure setting, the physical and textural liberation of aggregates converge towards the same value. This is explained by the secondary network invading the cement phase, as intense fracturing of the cement phase is necessary for single-particle impact breakage to yield liberated aggregates.

It was shown above that the strength of concrete decreased with microwave exposure, the same can be said of concrete stiffness. Textural image analysis showed an increase in the total crack length, total crack area and average crack width. This increase in crack width was significantly more pronounced in the primary network and specifically the aggregate/cement paste interface fractures. It is impossible to separate the effects of total fracture area and aggregate interface crack width on the mechanical properties as these two values increase together during microwave heating, but it has been noted that concrete stiffness is largely dependent on the ITZ (Mehta and Monteiro, 2005). In this work stiffness is measured with Hopkinson bar impact testing as defined by Tavares and King (Tavares and King, 1998). **Fig. 22** shows that as expected, the stiffness of the samples decreases rapidly with the increase in

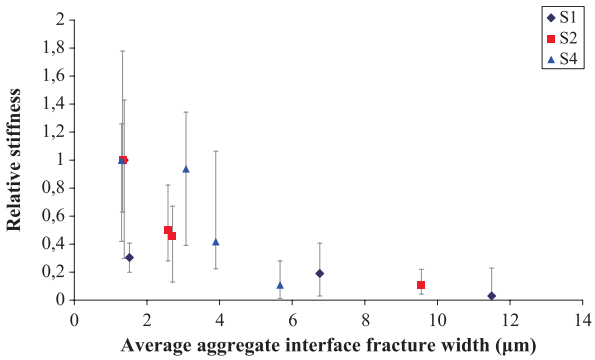

Fig. 22 Change in concrete stiffness with aggregate interface crack width.

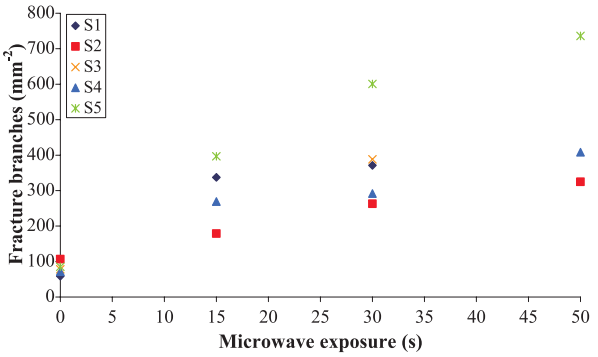

Fig. 24 Number of branches per cement area in secondary network.

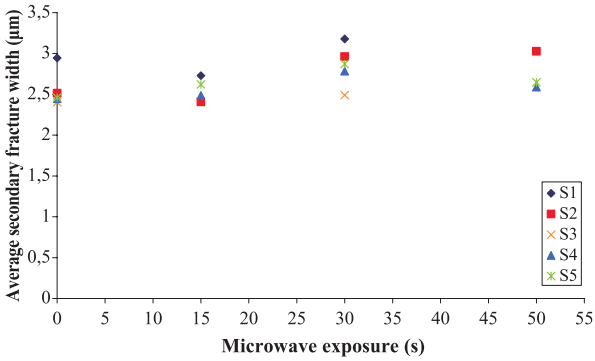

Fig. 23 Variations in secondary-network properties with microwave treatment time.

aggregate interface fracture width. The rate of change slows at higher temperatures, presumably as once aggregate and cement paste is separated the stiffness becomes dependent on the cement phase only, and increasing the size of this separation has no further effect. Similarly, concrete strength has been linked with porosity, the textural measure most analogous with porosity is the total crack area which increases steadily with microwave exposure and shows a strong correlation with loss of concrete strength and can be seen in **Fig. 21**. When compared with **Fig. 19**, it can be seen that the growth of the primary network can not be responsible for the strength loss in samples that have experienced a longer treatment, because while strength continues to decrease, the increase in primary-network fracture length slows with further microwave exposure.

Two-dimensional analysis of the fracture networks has a limited scope for understanding the way by which their properties correlate with operating conditions and with recycling performance indicators. Having clearly established that these fracture networks hold the key to concrete recyclability at the local scale, it appears that three-dimensional observation and analysis is the next logical step. Currently, X-ray tomography has a resolution that is fully compatible with that required to capture the primary network, at a resolution of say about 10 µm per voxel. The authors have started capturing tomographic images of 20-mm heated concrete samples, which confirm that the primary network is a highly connected network that percolates through heated concrete samples. On the other hand, capturing three-dimensional information about the secondary network is clearly more complex because the required resolution must be of the order of a micrometer or less. Nevertheless, the seemingly random occurrence of this network through the cement phase means that 3D properties of the secondary fracture network can possibly be inferred from 2D images using statistical means.

4.2 Analysis of the secondary network

The fracture network that forms during the microwave heating of concrete has been divided in two. The primary fracture network is associated with the aggregate grain boundary, and occurs with short exposure to microwaves, whereas the secondary network occurs randomly in the cement phase and spreads with increased exposure to microwave heating. Just as for the primary network, properties of interest of the secondary network include average properties such as total length, surface area and crack branch number, and statistical properties such as crack branch length, nodes, ends and width distributions. Contrary to the primary network fractures, **Figs. 23**, **24** shows that on average, cracks from the secondary network do not appear to grow wider with microwave treatment, but the total length and number of branches per unit area do increase with microwave heating time. The crack branch length distribution follows a log-normal distribution, as shown in **Fig. 25**, and does not change significantly between samples nor with increased heating duration. Put another way, the growth of individual fractures in the cement paste and the growth of the secondary fracture network as a whole occur together and in constant proportion. This is not unexpected as once the

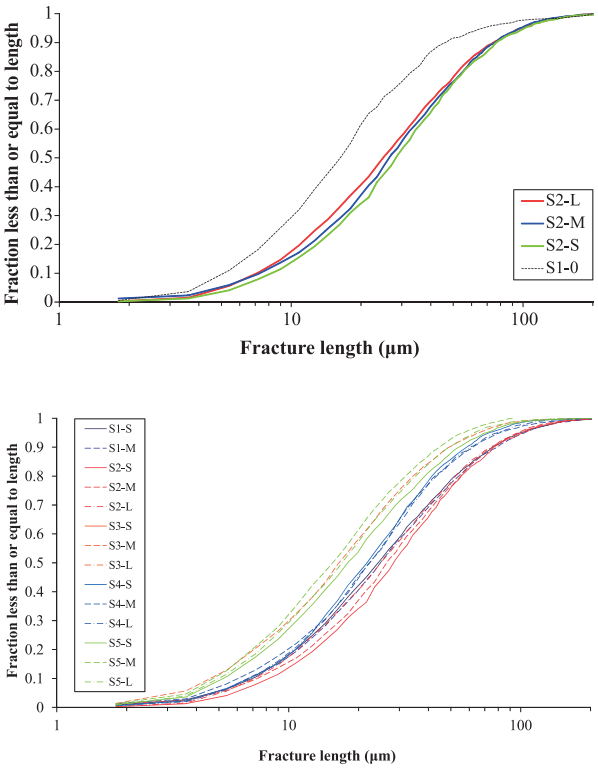

Fig. 25 Branch size distributions, secondary fracture network. Top: for sample S2. Bottom: for samples S1 to S5.

cement paste is disconnected from the aggregate, shrinkage is no longer constrained. This distribution is directly associated with the fineness of the fragments that form after comminution of the microwave-heated concrete samples. Additional research is required, however, in order to correlate the topological properties of the secondary network to the size distribution of the fragments obtained by comminution.

To finalise the discussion about the two fracture networks identified in this work, it was decided to take a look at their relative significance on properties of relevance to the recycling problem. As discussed earlier, the secondary crack length increases with microwave exposure time, i.e. with concrete energy absorption. **Fig. 26** shows the variation between total secondary network crack length relative to the total crack length and microwave exposure time. **Fig. 27** shows that while the total crack length increases steadily with increased microwave exposure, the rate of increase of the secondary-network crack length is faster, and is the key player in the loss of mechanical strength of microwave-heated concrete. As an illustration of this last point, **Fig. 28** shows the measured relationship between the secondary network total crack length relative to the total crack length and the strength of the concrete samples measured by HPB. The correlation is significant, with strength dropping almost in linear proportion to the increase in secondary network total crack length.

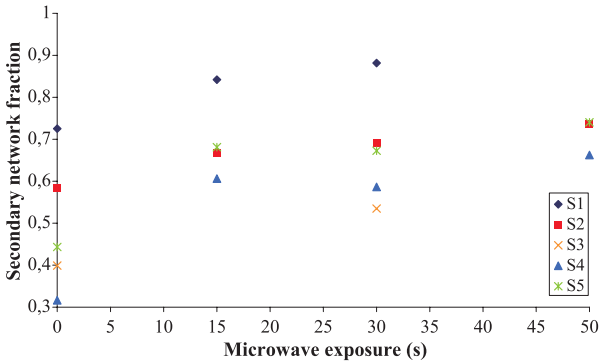

Fig. 26 Fraction of total crack length composed of secondary network.

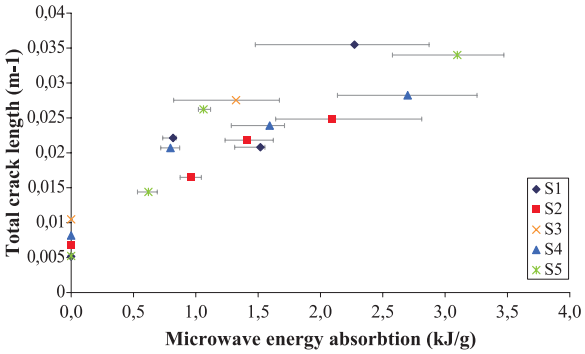

Fig. 27 Total combined crack length of primary and secondary network.

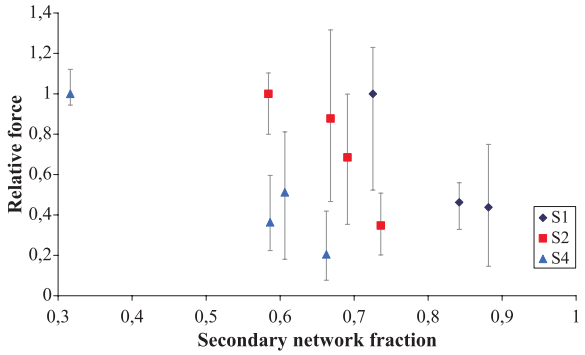

Fig. 28 Relative change in fracture force with fraction of total network length composed of secondary network.

5. Implications for development of a microwave -based concrete recycling process

This work, through local analysis of changes in the structure of porosity that occurs during the microwave heating of concrete, has added additional evidence to the body of existing knowledge about the potential value of microwave heating for the development of a concrete recycling process. The pattern of crack growth is evidence of drying shrinkage as it is the only crack formation mechanism to occur over the entire temperature range observed.

Importantly for concrete recycling, these results show that microwave heating causes fractures to occur at the aggregate/cement paste interface, and importantly for energy efficiency, these are the first microwave-induced fractures to form. Also of note is the observation that the properties of individual concretes are relatively unimportant. This will make the implementation of a microwave-based concrete recycling process easier as it will not require adaptation to different waste sources.

The analysis of fracture porosity has shown that microwave heating interacts strongly with the ITZ to generate a large-scale network of fractures at the aggregate/cement paste interface. Experimental results indicate that this primary network of fractures forms with a short exposure to microwaves. As previously stated, the most efficient microwave generators for embrittlement are those with the highest power output, however, this is based on the assumption that the key embrittlement mechanism is differential thermal expansion. It is still desired that the process is selective, and the higher the power of the microwave generator, the faster heating occurs, the less that conduction can play a role and the more selective the process is. Therefore a high-power generator is most likely still desirable but as dehydration appears to be the key mechanism in the microwave processing of concrete waste, one may expect the point at which increasing power output is no longer economical is lower than it would be for a similar application in mineral processing. In any case the technology needs to be perfected and the appropriate compromise found.

It was noted in a previous work (Lippiatt and Bourgeois, 2012) that the liberation of aggregate particles is seen only after extensive microwave treatment. This was measured using macro techniques, sample fracture then selective dissolution. Conversely, local techniques, i.e. SEM inspection of treated samples used in this work, show that fracture at the cement/aggregate interface occurs much earlier in the treatment process. What occurs later under extended microwave exposure is more extensive fracture growth throughout the cement paste. This extended cement crack growth greatly reduces the strength of the concrete sample and causes the sample to break into much smaller fragments when crushed under impact. It was due to this fragmentation in the cement paste that liberation was measured by impact fracture at such a high level for long-treated samples in this previous work, rather than any actual increase in the separation of the aggregate particles and cement paste.

The SEM results suggest that the aggregate and the cement were well separated, but unless an appropriate mechanical comminution technique is selected, the aggregate samples will remain encased within larger cement paste fragments. Development of an industrial solution would also require identification of an appropriate comminution process to exploit this primary network so as to close the gap between physical and textural liberation with minimum energy consumption.

The above discussion considers optimisation of the liberation of aggregates, and ignores other important dimensions of the process, towards which results from this work bring answers. Once comminution has taken place, a concrete's aggregate and cement paste would have to be separated. One possibility that can be inferred from this work's results would be to induce a dense secondary fracture network by microwave heating prior to comminution in order to generate cement fines, which could then easily be separated from liberated aggregates by dry screening. Moreover, reducing the cement paste to a fine powder would help facilitate the recycling of the cement paste. From these considerations, there is significant scope for development of a microwave-based recycling process, however, given that the microwave heating step is necessarily part of a processing chain that includes comminution, separation and transport, finding the right operating conditions is going to require additional research and development work.

6. Concluding remarks

The applicability of microwave heating to the recycling of concrete is an important issue, given the increase in demand for concrete, the scarcity of natural aggregate resources and the environmental footprint of clinker production. While a number of published works have shown the potential of developing a microwave-based recycling process based on macroscopic measurements relevant to concrete recycling performance, namely aggregate liberation, product fineness and mechanical embrittlement, this work establishes links between fracture porosity and observed macroscopic effects through local texture observation and analysis.

The work associates the formation of two fracture networks with specific recycling issues:

– The primary fracture network is constituted of large connected fractures that are associated with the aggregate grain boundaries, and occurs with short exposure to microwaves. This network, by essence, is responsible for the textural liberation of aggregates. The primary network appears to occur at the early stage of microwave heating.
– The secondary network is constituted of seemingly randomly occurring cracks which spread through the cement phase with increased exposure to microwave heating. This dense network of smaller fractures is strongly linked to the loss of mechanical strength of concrete, and the degree of actual physical liberation of aggregate particles obtained after impact fracture of microwave heated concrete samples.

Mechanisms responsible for the formation and growth of both primary and secondary fracture networks are undoubtedly complex, but the evidence from this work indicate that they are controlled by local drying shrinkage, which starts at the interfacial transition zone around aggregate particles and eventually spreads throughout the bulk of the cement matrix.

Capitalising on the high degree of textural liberation of aggregate particles obtained after a short microwave heating time only, meaning lower energy consumption, requires identification of a suitable comminution solution. The inefficiency of single-particle impact fracture to physically liberate aggregate particles that were texturally liberated suggests that impact-based comminution equipment is not the best option. It is thought that shear-inducing comminution technologies such as high-pressure grinding rolls should be investigated in conjunction with microwave heating.

The longer exposure to microwaves, however, yields extensive growth of secondary network fractures in the cement matrix and subsequent production of cement fines through comminution. Increased cement fines may be valuable for the separation of aggregates from cement and recycling of the cement itself as part of the overall recycling scheme.

In the end, it can be concluded that finding the best position and operating conditions for the microwave heating step in the concrete recycling chain is not a clear-cut situation. The setting of the microwave heating process to grow the primary and secondary fracture networks to a specific level depends on the subsequent process steps, including comminution, product separation and possibly transport.

Having looked at the local scale, one important conclusion from this work is that development of a microwave-based concrete recycling process must consider the processing chain in its entirety.

Acknowledgements

The authors acknowledge the financial support of the Agence Nationale de la Recherche (the French National Research Agency) through the COFRAGE project from the ECOTECH research programme. The authors want to acknowledge Dr. Emmanuel Cid, Senior Research Scientist with the Laboratoire de Génie Chimique, for his valuable contribution to the image analysis of the fracture patterns.

References

Akbarnezhad A., Ong K.C.G., Zhang M.H., Tam C.T., Foo T.W.J., Microwave-assisted beneficiation of recycled concrete aggregates, Construction and Building Materials, 25 (2011) 3469–3479.

Ali A.Y., Understanding the effects of mineralogy, ore texture and microwave power delivery on microwave treatment of ores, Ph.D. thesis, University of Stellenbosch, 2010.

Ben Haha M., Gallucci E., Guidom A.,Scrivener K.L., Relation of expansion due to alkali silica reaction to the degree of reaction measured by sem image analysis, Cement and Concrete Research, 37 (2007) 1206–1214.

Bourgeois F., Banini G., A portable load cell for in-situ ore impact breakage testing, International Journal of Mineral Processing, 6 (2002) 31–54.

Brough A.R., Atkinson A., Automated identification of the aggregate–paste interfacial transition zone in mortars of silica sand with portland or alkali-activated slag cement paste, Cement and Concrete Research, 30 (2000) 849–854.

Costes J.R., Majcherczyk C., Binkhorst I.P., Total recycling of concrete, Commissariat à l'Énergie Atomique, online publication, 2010.

Diamond S., Mercury porosimetry an inappropriate method for the measurement of pore size distributions in cement-based materials, Cement and Concrete Research, 30 (2000) 1517–1525.

Figg J., Microwave heating in concrete analysis, Journal of Applied Chemistry and Biotechnology, 24 (1974) 143–155.

Fischer C., Davidsen C., Europe as a recycling society, Report for the European Environment Agency, 2011.

Igarashi S., Kawamura M., Watanabe A. Analysis of cement pastes and mortars by a combination of backscatter-based SEM image analysis and calculations based on the powers model, Cement and Concrete Composites, 26 (2004) 977–985.

Jerby E., Dikhtyar V., Aktushev O., Grosglick U., The microwave drill, Science, 298 (2002) 587–589.

Kingman S.W., Jackson W., Bradshaw S.M., Rowson N.A., An investigation into the influence of microwave treatment on mineral ore comminution, Powder Technology, 146 (2004a) 176–184.

Kingman S.W., Jackson K., Cumbane A., Bradshaw S.M., Rowson N.A., Greenwood R., Recent developments in microwave assisted comminution, International Journal of Mineral Processing, 74 (2004b) 71–83.

Kiss L., Shönert K., Liberation of two component material by single particle compression and impact crushing, Aufbereit.-Tech, 30 (1980) 223–230.

Klee H., The cement sustainability initiative, Progress report for the World Business Council for Sustainable Development, Duesseldorf, Geneva, 4 June 2009.

Lippiatt N., Bourgeois F., Investigation of microwave-assisted concrete recycling using single-particle testing, Minerals Engineering, 31 (2012) 71–81.

Mehta P., Monteiro P., Concrete: microstructure, properties and materials, 3rd Revised edition, McGraw-Hill Professional, 2005.

Piasta J., Sawicz Z., Rudzinski L., Changes in the structure of hardened cement paste due to high temperature, Matériaux et Constructions, 17 (1984) 291–296.

Roy D.M., Idorn G.M., Concrete microstructure, Strategic Highway Research Program, National Research Council, Washington, DC, 1993.

Symonds Group, Construction and demolition waste

management practices and their economic impacts, Report for the European Commission in association with ARGUS, COWI and PRC Bouwcentrum, 1999.

Tam V.W.Y., Tam C.M., Wang Y., Optimization on proportion for recycled aggregate in concrete using two-stage mixing approach, Construction and Building Materials, 21 (2007) 1928–1939.

Tavares L.M., King R.P., Single-particle fracture under impact loading. International Journal of Mineral Processing, 54 (1998) 1–28.

White T.L., Foster D.J., Wilson C.T., Schaich R., Phase II microwave concrete decontamination results, Oak Ridge National Laboratory, 1995.

Wong H.S., Head M.K., Buenfeld N.R., Pore segmentation of cement-based materials from backscattered electron images, Cement and Concrete Research, 36 (2006) 1083–1090.

Yang R., Buenfeld N.R., Binary segmentation of aggregate in SEM image analysis of concrete, Cement and Concrete Research, 31 (2001) 437–441.

Author's short biography

Nicholas Lippiatt

Nicholas Lippiatt holds a masters in materials science (France) and completed his bachelor's degree in materials engineering at the University of Queensland in Brisbane, Australia. He is currently completing a Ph.D. in materials science (Laboratoire de Génie Chimique, Institut National Polytechnique de Toulouse) in France on the use of microwave heating technology for concrete recycling.

Florent Bourgeois

Prof. Bourgeois holds a B.Eng. in materials science (France) and a Ph.D. in extractive metallurgy (University of Utah). He worked as a research fellow for the CRC Mining (Australia) from 1994 to 1996, and as a lecturer in minerals processing with the University of Queensland from 1997 until 2000. Between 2001 and 2005, he worked as project leader for the French Geological Survey's processing department. He now holds a tenured position at the University of Toulouse. His field of expertise is particulate process design and modelling, with emphasis on comminution, liberation, texture modelling, sampling of minerals and wastes.